Near-field Imaging and Diagnostics for Antennas and Radomes

Mats Gustafsson

Department of Electrical and Information Technology, Lund University, Sweden

Seoul National University, Seoul, Korea, 2017-04-20

Outline

1. **Acknowledgments & Lund University**
2. **Motivation**
3. **Radome and Antenna diagnostics**
   - Inverse source problem
   - Inversion algorithm
   - Radome diagnosticss
4. **Compressive sensing**
5. **Conclusions**

Acknowledgments

- IEEE APS Distinguished Lecturer Program
- Sweden's innovation agency (VINNOVA)
- Swedish Foundation for Strategic Research (SSF)

Collaboration with:

- Kristin Persson, PhD 2013 from LU
- Jakob Helander, LU
- Andreas Ericsson, LU
- Gerhard Kristensson, LU
- Björn Widenberg, GKN
- Daniel Sjöberg, LU
- Christer Larsson, SAAB
- Torleif Martin, SAAB

Swedish Foundation for Strategic Research

Lund University

- Lund university was founded in 1666.
- Sweden's largest university.
- Approximately 40 000 students.
- Department of Electrical and Information Technology: Broadband Communications, Circuits and Systems, Communication, Electromagnetic theory, Networking and Security, Signal Processing.

Outline

1. **Acknowledgments & Lund University**
2. **Motivation**
3. **Radome and Antenna diagnostics**
    - Inverse source problem
    - Inversion algorithm
    - Radome diagnosticss
4. **Compressive sensing**
5. **Conclusions**

Antennas

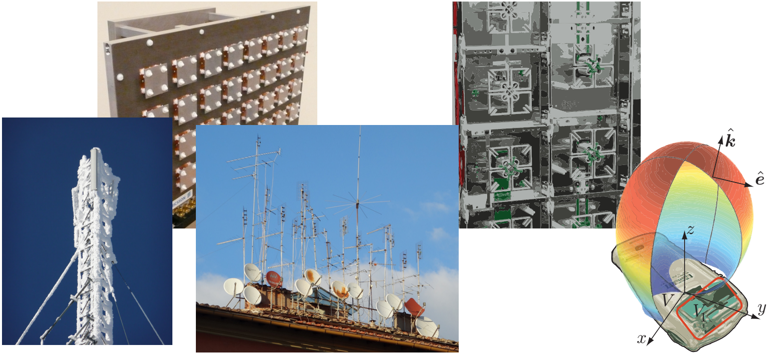

- Antennas radiate (or receive) electromagnetic waves.
- Usually characterized by the impedance (S-parameters) and radiation pattern (gain, realized gain, cross polarization,...).
- Defects (*e.g.*, malfunctioning elements) affect these parameters in a complex way.

Radomes

- A radome encloses an antenna to protect it from, *e.g.*, environmental influences.
- Ideally electrically transparent.
- Often reduces gain and increases side-lobe levels.
- Flash (image) lobes from reflections of the radome wall.

Localization of defects

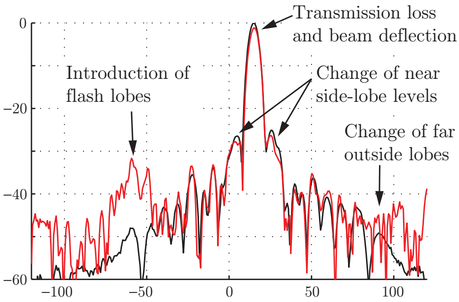

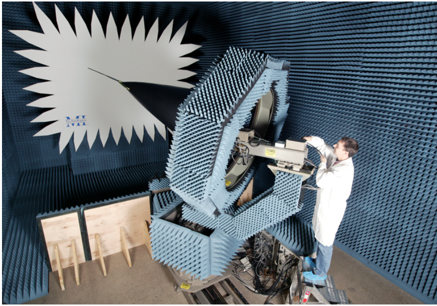

- Defects in antennas (in elements, feed structure) and radomes affect the impedance and radiated field in a complex way.
- The small localized defect can perturb the radiation pattern (for all angles). Can be difficult to correlate with the location of the defect.
- Near field and/or equivalent currents can localize defects.

Imaging of fields and currents

Measurements and simulations

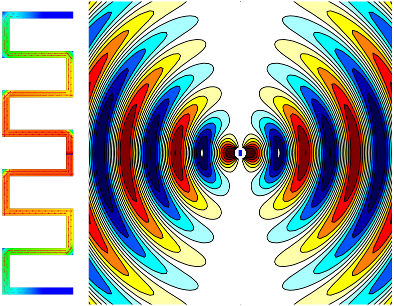

- In addition to antenna parameters, EM simulations provide images of the current and field distribution.
- Very useful for understanding and intuition.
- Would be as useful to obtain similar information from measurements...

Imaging of fields and currents

Measurements and simulations

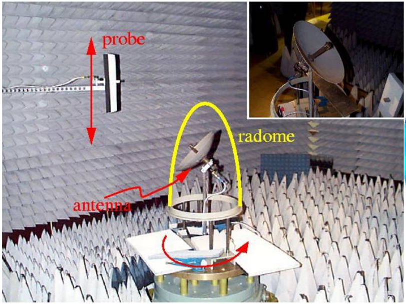

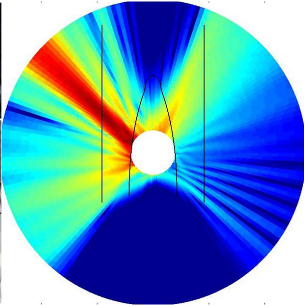

- In addition to antenna parameters, EM simulations provide images of the current and field distribution.
- Very useful for understanding and intuition.
- Would be as useful to obtain similar information from measurements...

EM source reconstruction

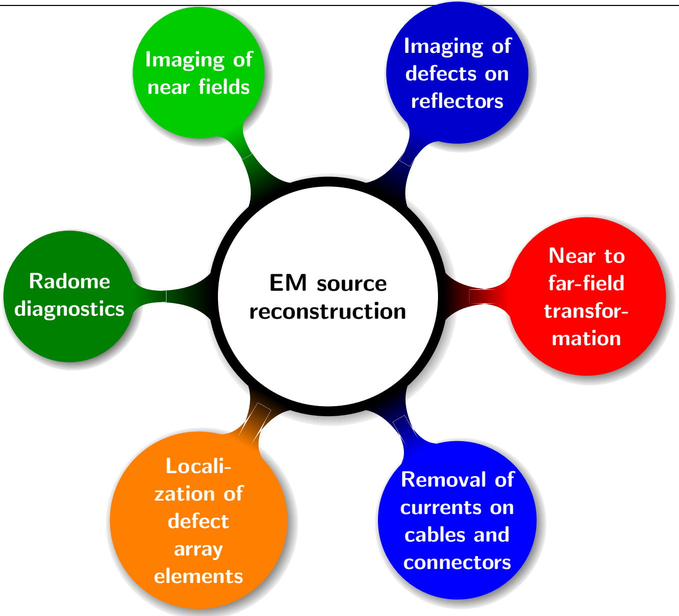

Outline

1. Acknowledgments & Lund University
2. Motivation
3. **Radome and Antenna diagnostics**
   - Inverse source problem
   - Inversion algorithm
   - Radome diagnosticss
4. Compressive sensing
5. Conclusions

Radome and antenna diagnostics using near/far-field data

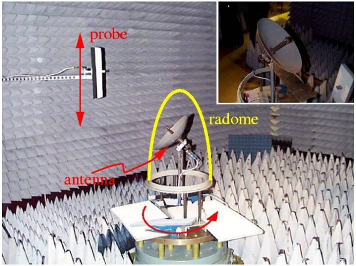

Cylindrical near-field measurements.

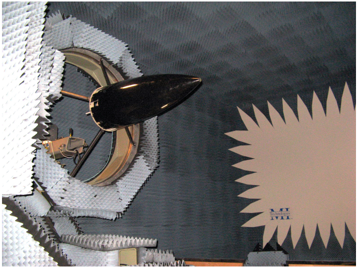

Compact range far-field measurements.

- Radomes affect the radiated field.
- Reconstruct the EM-fields on a surface to localize defects.
- Inverse source problems (ill-posed).
- Amplitude and phase in near- or far-field data.
- Analytic results for planar and spherical geometries.
- Integral equations and integral representations for arbitrary geometries.

Some background

Antenna/radome diagnostics is intimately tied to the development of measurement technology and can be characterized by the measurement geometry, computational method, and purpose. Inverse source problem with analysis of non-radiating currents and regularization.

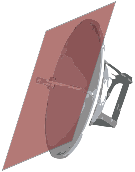

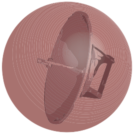

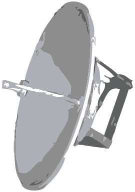

- **Measurement geometry:** near- and far-field, planar (rectangular, polar, bi-polar), cylindrical, and spherical.
- **Method:** field expansion (plane waves, cylindrical, spherical), back propagation (phase conjugation/time reversal, microwave holography), and inversion (integral representation).
- **Purpose:** diagnostics and/or near- to far-field transformation.

Some references:

- Barrett & Barnes, Automatic antenna wavefront plotter, 1952.
- Bleistein & Cohen, Nonuniqueness in the inverse source problem in acoustics and electromagnetics, 1977.
- Rahmat-Samii, Surface diagnosis of large reflector antennas using microwave holographic metrology, 1984.
- Yaghjian, An Overview of Near-Field Antenna Measurements, 1986.
- Hansen, Spherical near-field antenna measurements, 1988.
- Slater, Near-Field Antenna Measurements, 1991.
- Rahmat-Samii *etal*, The UCLA Bi-Polar Planar Near Field Antenna Measurement and Diagnostics Range, 1995.
- Sarkar & Taaghol, Near-field to near/far-field transformation for arbitrary near-field geometry, utilizing an equivalent magnetic current, 1996.
- Hansen, Discrete Inverse Problems: Insight and Algorithms, 2010.
- Devaney, Mathematical foundations of imaging, tomography and wavefield inversion, 2012.

Inverse source problems/diagnostics background

- Plane wave spectrum at least 1950 Barrett & Barnes, see also *e.g.*, Devany, Joy, Hansen, Yaghijian, Wang, Sarkar, Rahmat-Samii, ...
- Modal expansion (spherical, cylindrical, spheroidal) at least 70's, see *e.g.*, Devany, Hansen, Guler, Joy, Sten, Marengo, Ziyyat,Cappellin, Breinbjerg, Frandsen,...
- Integral representation (MoM)
  - 2001 Laurin *etal*: $\boldsymbol{M}$ *on planar structures.*
  - 2005 Persson & Gustafsson: *BoR using the extinction theorem for radome applications.*
  - 2006 Las-Heras *etal*: $\boldsymbol{J}$ *and* $\boldsymbol{M}$ *on antennas without the extinction theorem*.
  - 2009 Eibert *etal*: *Fast multipole and higher order basis functions.*
  - 2009 Araque Quijano & Vecchi: *3D structures using a dual formulation (extinction theorem).*
  - 2010 Jögensen *etal*: antenna diagnostics.
  - 2011 Araque Quijano *etal*: *post-processing to remove disturbances.*
  - 2011 *Commercial packages:* Diatool by TICRA and Insight by Satimo.

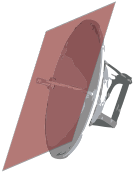

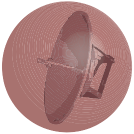

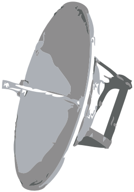

Inverse source problems

Inverse problem

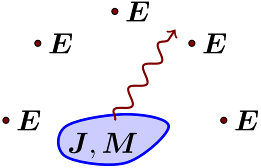

Inverse source problem. Determine the sources $(\boldsymbol{J}, \boldsymbol{M})$ in a region from observation of the field $\boldsymbol{E}$ in some points.

Back propagation

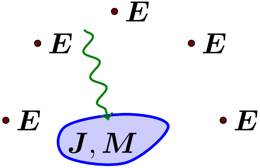

Use the data as sources and retransmit the field (time reversal or phase conjugation). Robust classical approach.

Inversion

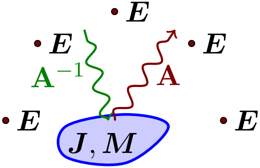

Find the source distribution from the linear system

$$\mathbf{A}\mathbf{x} = \mathbf{b}$$

with

- $\mathbf{x}$ as $\boldsymbol{J}, \boldsymbol{M}$
- $\mathbf{b}$ as $\boldsymbol{E}, \boldsymbol{H}$

Inverse source problems

Determine the current distribution from measurements of the radiated field

Volume currents

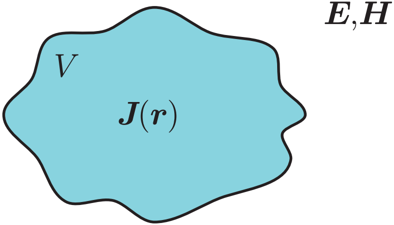

- Electric current density $\boldsymbol{J}(\boldsymbol{r})$ in the volume V. (Also magnetic currents.)
- Non-unique.
- Non-radiating currents.

Equivalent surface currents

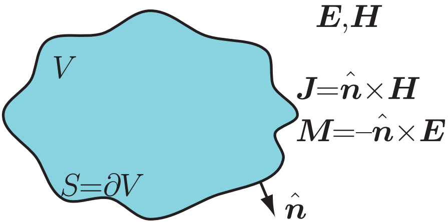

- Equivalent electric and magnetic surface current densities $\boldsymbol{J},\boldsymbol{M}$ on the surface $S=\partial V$.
- Non-unique.
- Equivalence principle.

Inversion algorithm (outline of the derivation) I

The electric fields at the position $\boldsymbol{r}$ from the electric surface current $\boldsymbol{J}$ on $S = \partial V$ is

$$\boldsymbol{E}(\boldsymbol{r}) = -\mathcal{L}\left(\eta_0 \boldsymbol{J}\right)(\boldsymbol{r})$$

were (free space Green's function G)

$$\mathcal{L}(\boldsymbol{X})(\boldsymbol{r}) = \mathrm{j}k \int_S G(\boldsymbol{r}-\boldsymbol{r}')\boldsymbol{X}(\boldsymbol{r}') - \frac{1}{k^2}\ \nabla' G(\boldsymbol{r}-\boldsymbol{r}')\nabla'_{\mathrm{S}} \cdot \boldsymbol{X}(\boldsymbol{r}')\,\mathrm{dS}'$$

and from the magnetic surface current $\boldsymbol{M}$ we have

$$\boldsymbol{E}(\boldsymbol{r}) = \mathcal{K}\left(\boldsymbol{M}\right)(\boldsymbol{r})$$

where

$$\mathcal{K}(\boldsymbol{X})(\boldsymbol{r}) = \int_S \nabla' G(\boldsymbol{r}-\boldsymbol{r}') \times \boldsymbol{X}(\boldsymbol{r}')\,\mathrm{dS}'$$

Inversion algorithm (outline of the derivation) II

Consider a measured electric field, $\boldsymbol{E}_{\text{meas}}(\boldsymbol{r}_n)$, in the points $\boldsymbol{r}_n$ and the polarization $\hat{\boldsymbol{e}}_n$, where $n = 1, ..., N$ and N is the number of measurement points.

The integral representation relates the surface currents to the measured fields

$$\hat{\boldsymbol{e}}_n \cdot \Big(-\mathcal{L}\left(\eta_0 \boldsymbol{J}\right)(\boldsymbol{r}_n) + \mathcal{K}\left(\boldsymbol{M}\right)(\boldsymbol{r}_n) \Big) = \hat{\boldsymbol{e}}_n \cdot \boldsymbol{E}_{\text{meas}}(\boldsymbol{r}_n)$$

for all points $n = 1, ..., N$.
We can now expand the surface currents $\boldsymbol{J}, \boldsymbol{M}$ in basis function to get a linear system that can be solved to estimate $\boldsymbol{J}, \boldsymbol{M}$.

- We could also assume that $\boldsymbol{M} = \mathbf{0}$ and only solve for $\boldsymbol{J}$.
- Or any linear combination between $\boldsymbol{M}$ and $\boldsymbol{J}$.
- Can we do better?

Inversion algorithm (outline of the derivation) III

Assume a reconstruction surface S that surrounds the volume V and do not intersect ∂V. This implies that the source of the radiated field is inside of S.

The electric $\boldsymbol{E}$ and magnetic $\boldsymbol{H}$ fields outside S can be represented with the equivalent currents $\boldsymbol{M} = -\hat{\boldsymbol{n}} \times \boldsymbol{E}$ and $\boldsymbol{J} = \hat{\boldsymbol{n}} \times \boldsymbol{H}$ on the surface S.

Integral representation to relate the equivalent currents to the fields

$$-\mathcal{L}\left(\eta_0 \boldsymbol{J}\right)(\boldsymbol{r}) + \mathcal{K}\left(\boldsymbol{M}\right)(\boldsymbol{r}) = \begin{cases} \boldsymbol{E}(\boldsymbol{r}) & \boldsymbol{r} \text{ outside } S \\ \boldsymbol{0} & \boldsymbol{r} \text{ inside } S \end{cases}$$

Also a corresponding representation for the magnetic field.

- first equation for the measured field.
- second equation to relate $\boldsymbol{J}$ and $\boldsymbol{M}$ at S.

Removes the ambiguity in $\boldsymbol{J}, \boldsymbol{M}$ and produces equivalent currents that correspond to the true $\boldsymbol{E}, \boldsymbol{H}$ fields outside S.

Inversion algorithm (summary)

Integral equation EFIE (or MFIE, CFIE) on the reconstruction surface S with unit normal $\hat{\boldsymbol{n}}$

$$\hat{\boldsymbol{n}}(\boldsymbol{r}) \times \Big(\mathcal{L}\left(\eta_0 \boldsymbol{J}\right)(\boldsymbol{r}) - \mathcal{K}\left(\boldsymbol{M}\right)(\boldsymbol{r})\Big) = \frac{1}{2}\boldsymbol{M}(\boldsymbol{r}) \qquad \boldsymbol{r} \in S$$

and integral representation to relate the equivalent currents to the measured fields

$$\hat{\boldsymbol{e}}_n \cdot \Big(-\mathcal{L}\left(\eta_0 \boldsymbol{J}\right)(\boldsymbol{r}_n) + \mathcal{K}\left(\boldsymbol{M}\right)(\boldsymbol{r}_n)\Big) = \hat{\boldsymbol{e}}_n \cdot \boldsymbol{E}_{\mathrm{meas}}(\boldsymbol{r}_n)$$

for $n = 1, ..., N$ (number of measurement points), where (again)

$$\begin{cases} \mathcal{L}(\boldsymbol{X})(\boldsymbol{r}) = \mathrm{j}k \displaystyle\int_S G(\boldsymbol{r}', \boldsymbol{r})\boldsymbol{X}(\boldsymbol{r}') - \frac{1}{k^2}\,\nabla' G(\boldsymbol{r}', \boldsymbol{r})\nabla'_{\mathrm{S}} \cdot \boldsymbol{X}(\boldsymbol{r}')\,\mathrm{dS}' \\ \mathcal{K}(\boldsymbol{X})(\boldsymbol{r}) = \displaystyle\int_S \nabla' G(\boldsymbol{r}', \boldsymbol{r}) \times \boldsymbol{X}(\boldsymbol{r}')\,\mathrm{dS}' \end{cases}$$

Gives an ill-posed linear system. Expand in basis functions to get an ill-conditioned matrix equation $\mathbf{A}\mathbf{x} = \mathbf{b}$.

Linear inverse problems

Would like to solve

$$\mathbf{A}\mathbf{x} = \mathbf{b}$$

with the $M \times N$ matrix $\mathbf{A}$. Simple to solve if $M = N$ and cond$A$ not too large (compared with the errors and noise in $\mathbf{A}$ and $\mathbf{b}$). Otherwise

- SVD: $\mathbf{A} = \mathbf{U}\mathbf{\Sigma}\mathbf{V}^{\mathsf{H}}$ with $\mathbf{U}^{\mathsf{H}}\mathbf{U} = \mathbf{I}$ and $\mathbf{V}^{\mathsf{H}}\mathbf{V} = \mathbf{I}$
- $\mathbf{L}^2$-minimization: $\|\mathbf{x}\|_2 = (\sum_{n=1}^{N} |x_n|^2)^{1/2}$
- $\mathbf{L}^1$-minimization: $\|\mathbf{x}\|_1 = \sum_{n=1}^{N} |x_n|$
- $\mathbf{L}^0$-minimization: the number of non-zero entries of $\mathbf{x}$. (not a norm)
- Regularization

SVD and $\mathbf{L}^2$ have many similarities. Would like to use $\mathbf{L}^0$ in compressive sensing but approximate with $\mathbf{L}^1$ to form convex optimization problems. Can use CVX for small problems and dedicated solvers (TFOCS, spgl1,...) for larger size problems (matrix free).

$\mathbf{L}^2$-inversion and regularization

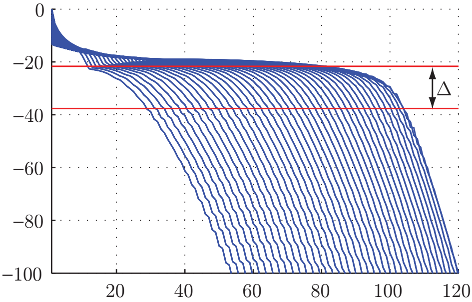

- The inverse source problem is ill-posed, *i.e.*, small errors in the data can produce large errors.
- Need regularization, *e.g.*, Tikhonov, SVD.
- The approximate matrix equation is ill-conditioned.
- Here, we use singular value decomposition (SVD).
- The regularization parameter is chosen in a calibration step.
- L-curve for automated regularization.

Radome diagnostics setup

- The electric field is measured (sampled) in a discrete set of points $\hat{\boldsymbol{e}}_n \cdot \boldsymbol{E}_{\text{meas}}(\boldsymbol{r}_n)$.
- Here, we use cylindrical near or spherical far-field setups.
- Probe compensation is not needed for the far-field measurements.
- Estimate the field (equivalent currents) on the radome surface.

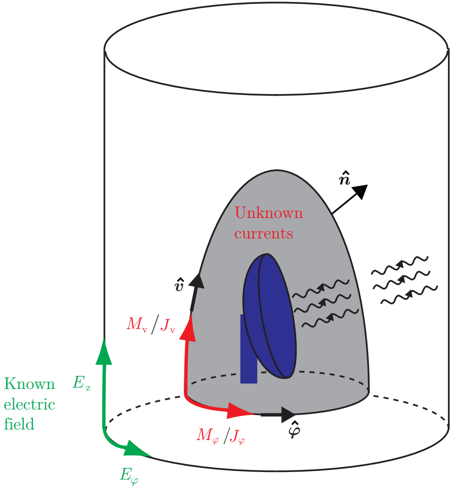

Radome diagnostics setup

- The electric field is measured (sampled) in a discrete set of points $\hat{\boldsymbol{e}}_n \cdot \boldsymbol{E}_{\mathrm{meas}}(\boldsymbol{r}_n)$.
- Here, we use cylindrical near or spherical far-field setups.
- Probe compensation is not needed for the far-field measurements.
- Estimate the field (equivalent currents) on the radome surface.

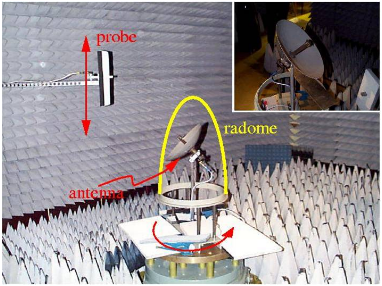

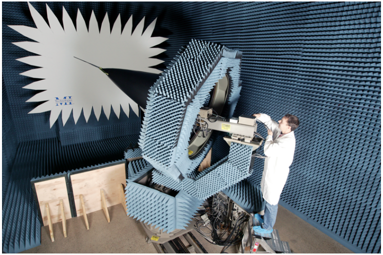

Phase image of a dielectric radome

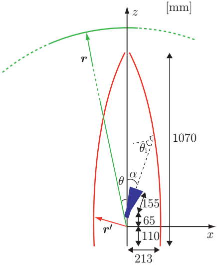

Compact range far-field measurements.

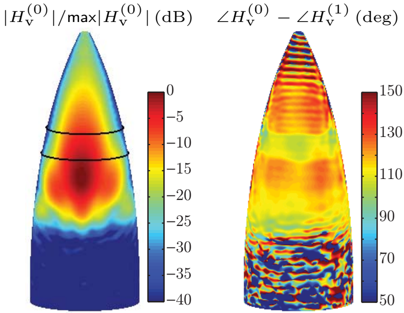

Radome diagnostics.

- Measured data from ACAB's compact far-field range*.
- Dielectric radome with height $1.07\,\mathrm{m} \approx 36\lambda$ at $10\,\mathrm{GHz}$.
- Phase image of the radome wall.

Persson+etal, Radome diagnostics - source reconstruction of phase objects with an equivalent currents approach, IEEE-TAP, 2014.

*GKN Aerospace Applied Composites, Linkping, Sweden.

Measurement configurations

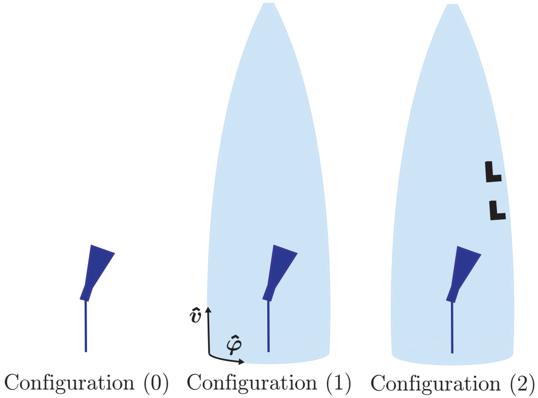

Initially three measurement configurations:

0. without radome.
1. with radome.
2. with defect radome.

Imaging of dielectric tape on a radome

Radome with dielectric patches

Amplitude
$|H_{\mathrm{v}}^{(1)}|/\mathrm{max}|H_{\mathrm{v}}^{(1)}|\,(\mathrm{dB})$

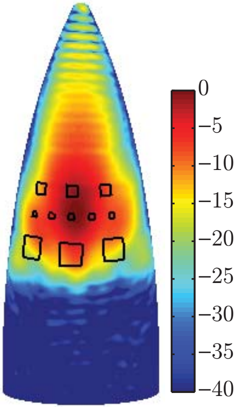

Phase
$\angle H_{\mathrm{v}}^{(1)} - \angle H_{\mathrm{v}}^{(2)}\,(\mathrm{deg})$

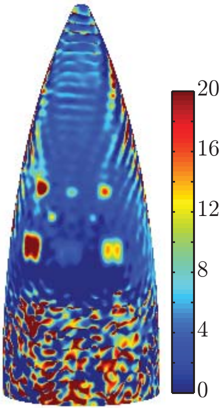

Imaging of dielectric tape on a radome

1 to 8 layers of tape

$\angle H_{\mathrm{v}}^{(1)} - \angle H_{\mathrm{v}}^{(2)}$ (deg)

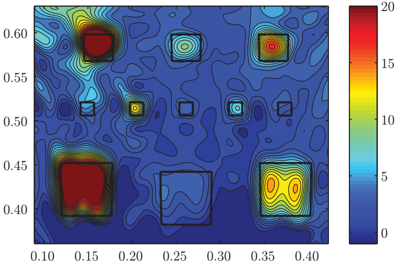

- Scotch Glass Cloth Electrical Tape 69-1 with thickness $\approx 0.15\,\mathrm{mm}$, $\epsilon_{\mathrm{r}} \approx 4.1$, and phase shift 1° to 2° (used to trim dielectric radomes).
- Squares with sides of $\{15, 30, 60\}\,\mathrm{mm}$. 1 to 8 layers.
- Measurements at $10\,\mathrm{GHz}$, $\lambda \approx 30\,\mathrm{mm}$.

Imaging of dielectric tape on a radome

Radome with dielectric LU

Amplitude $|H_{\mathrm{v}}^{(1)}|/\max|H_{\mathrm{v}}^{(1)}|\,(\mathrm{dB})$

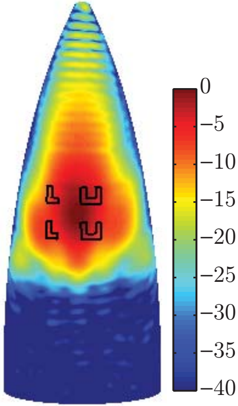

Phase $\angle H_{\mathrm{v}}^{(1)} - \angle H_{\mathrm{v}}^{(2)}\,(\mathrm{deg})$

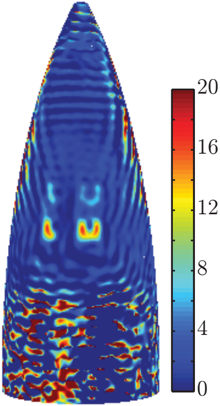

Imaging of dielectric tape on a radome

Radome with dielectric LU

Amplitude $|H_{\mathrm{v}}^{(1)}|/\max|H_{\mathrm{v}}^{(1)}|\,(\mathrm{dB})$

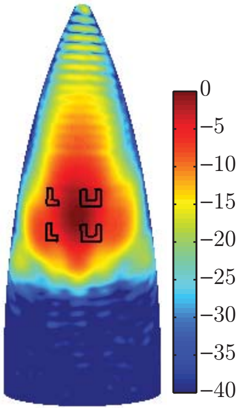

Phase $\angle H_{\mathrm{v}}^{(1)} - \angle H_{\mathrm{v}}^{(2)}\,(\mathrm{deg})$

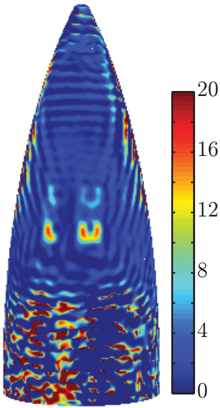

E and H fields

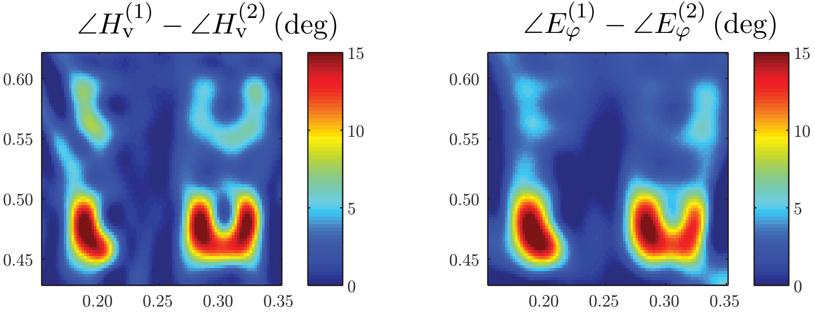

- We mainly image the H-fields.
- It is noted that the H-field images are better than the E-field images.
- Simulation using CST for a thin dielectric patch.
- Can be due to the dominant electric reactive near field from the dielectric patches.

E and H fields

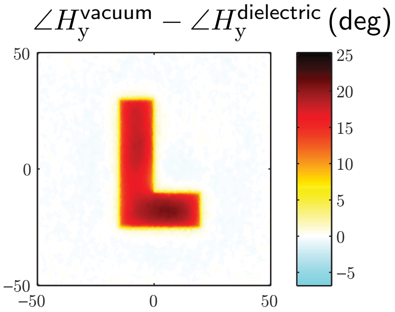

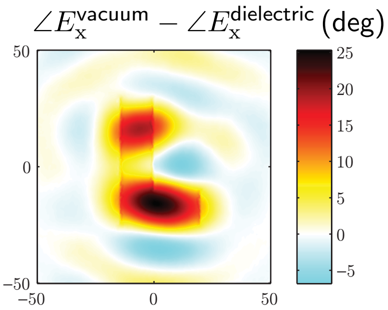

- We mainly image the H-fields.
- It is noted that the H-field images are better than the E-field images.
- Simulation using CST for a thin dielectric patch.
- Can be due to the dominant electric reactive near field from the dielectric patches.

FSS radome

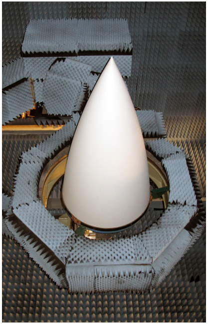

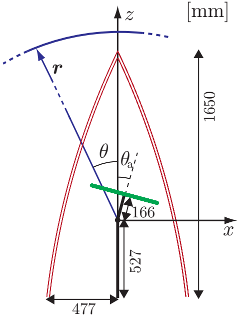

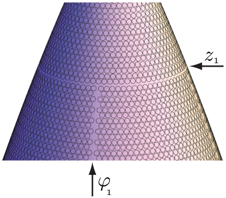

- Frequency selective radome with a passband around $9\,\mathrm{GHz}$.
- Disturbances in the lattice due to the double curvature of the radome surface. Here, line defects.
- Radome with height $1.65\,\mathrm{m} \approx 51\lambda$ at $9.35\,\mathrm{GHz}$.

Persson *etal*, Source reconstruction by far-field data for imaging of defects in frequency selective radomes, IEEE AWPL, 12, 480-483, 2013.

H-field on the FSS

- Amplitude difference between radome and without radome.
- (left) v-, (right) ϕ-component.
- (top) antenna roll $\phi = 0°$, (bottom) $\phi = 20°$.
- Normalized with maximal value.

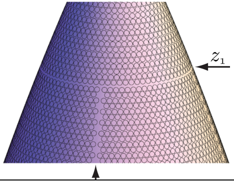

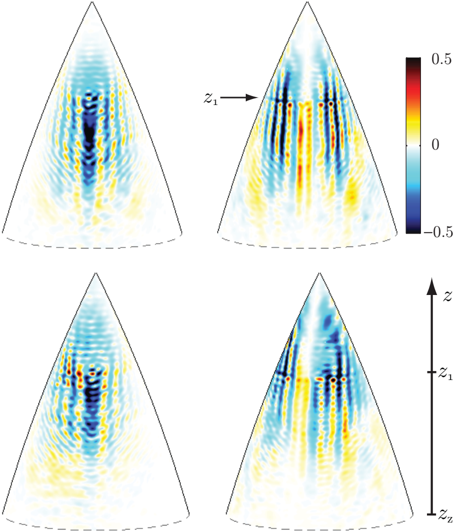

Power flow on the FSS

- Power flow difference between radome and without radome.
- Antenna roll $\phi = 0$.
- Normalized with maximal value (left) pointwise (right).

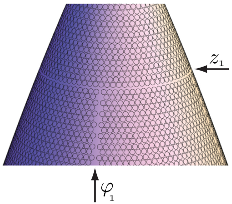

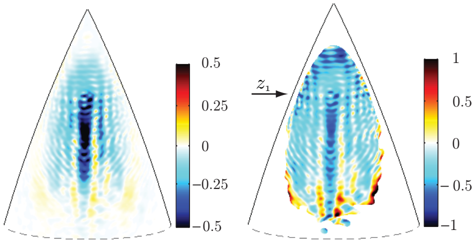

Diagnostics

- Near field and/or equivalent currents can localize defects.
- Imaging of the fields and/or equivalent currents for understanding.
- Integral equations (similar to MoM).
- One drawback is the measurement time. Can take several hours to measure the near/far field around the structure.
- Defects are often localized and there are often only a few defects.
- Utilize the sparse image (few defects) to improve the image quality and reduce the measurement time.
- Compressive sensing.

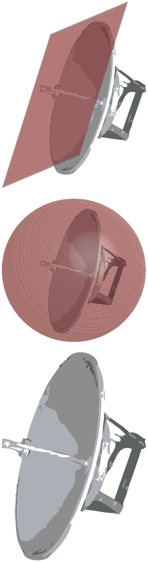

Outline

1. **Acknowledgments & Lund University**
2. **Motivation**
3. **Radome and Antenna diagnostics**
   - Inverse source problem
   - Inversion algorithm
   - Radome diagnosticss
4. **Compressive sensing**
5. **Conclusions**

Inverse source problems

Inverse problem

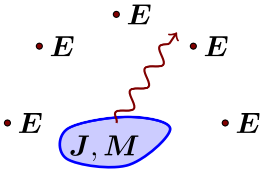

Inverse source problem. Determine the sources $(\boldsymbol{J}, \boldsymbol{M})$ in a region from observation of the field $\boldsymbol{E}$ in some points.

Back propagation

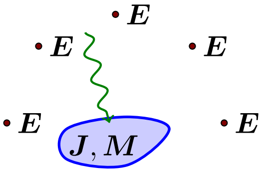

Use the data as sources and retransmit the field (time reversal or phase conjugation). Robust classical approach.

Inversion

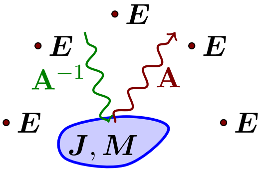

Find the source distribution from the linear system

$$\mathbf{A}\mathbf{x} = \mathbf{b}$$

with

- $\mathbf{x}$ as $\boldsymbol{J}, \boldsymbol{M}$
- $\mathbf{b}$ as $\boldsymbol{E}, \boldsymbol{H}$

Linear inverse problems

Would like to solve

$$\mathbf{A}\mathbf{x} = \mathbf{b}$$

with the $M \times N$ matrix $\mathbf{A}$. Simple to solve if $M = N$ and cond$A$ not too large (compared with the errors and noise in $\mathbf{A}$ and $\mathbf{b}$). Otherwise

- SVD: $\mathbf{A} = \mathbf{U}\mathbf{\Sigma}\mathbf{V}^{\mathsf{H}}$ with $\mathbf{U}^{\mathsf{H}}\mathbf{U} = \mathbf{I}$ and $\mathbf{V}^{\mathsf{H}}\mathbf{V} = \mathbf{I}$
- $\mathbf{L}^2$-minimization: $\|\mathbf{x}\|_2 = (\sum_{n=1}^{N} |x_n|^2)^{1/2}$
- $\mathbf{L}^1$-minimization: $\|\mathbf{x}\|_1 = \sum_{n=1}^{N} |x_n|$
- $\mathbf{L}^0$-minimization: the number of non-zero entries of $\mathbf{x}$. (not a norm)
- Regularization

SVD and $\mathbf{L}^2$ have many similarities. Would like to use $\mathbf{L}^0$ in compressive sensing but approximate with $\mathbf{L}^1$ to form convex optimization problems. Can use CVX for small problems and dedicated solvers (TFOCS, spgl1,...) for larger size problems (matrix free).

Rectangular region with local basis functions

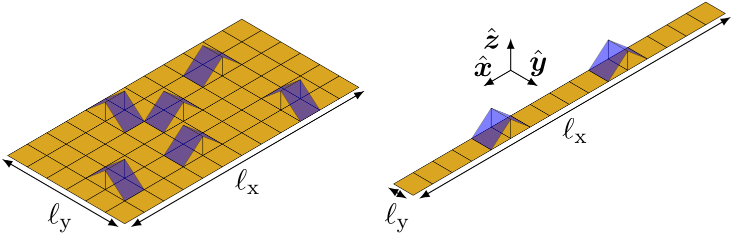

Consider a planar rectangle in the $z = 0$ plane. The rectangle is divided into $N_{\mathrm{x}} \times N_{\mathrm{y}}$ elements and the current density is expanded in basis functions.

The electric field is evaluated in N points (and polarizations). The electric field is expressed as $\mathbf{b} = \mathbf{A}\mathbf{x}$.

Sampled field from 2 point sources

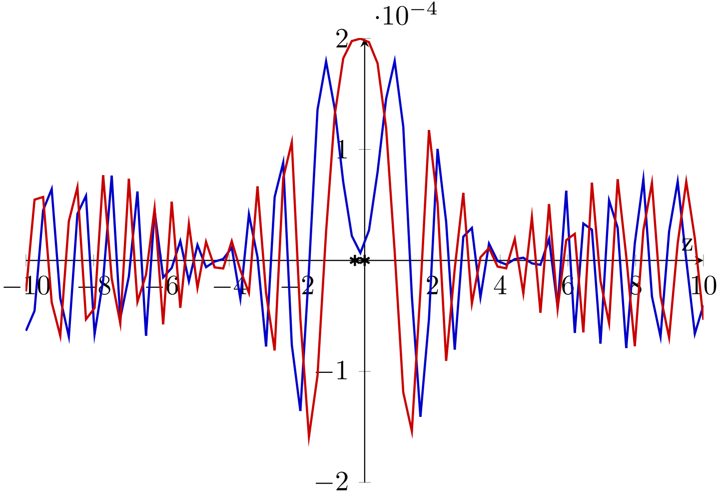

SVD 1D case with $M = 80$ and $N = 89$

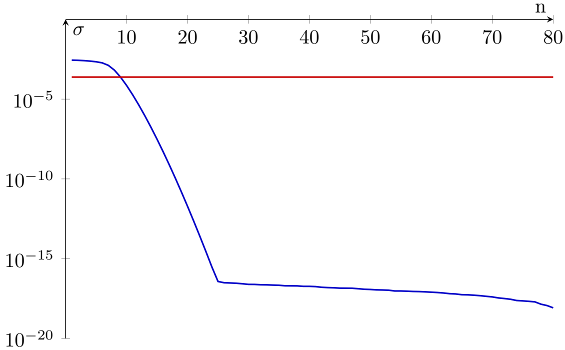

The singular values show a few dominant components (≈ 10), an exponential decay (evanescent components), and a noise level around 10^{-16}. Can only determine ≈ 10 out of the 89 unknowns. The remaining (≈ 79) degrees of freedom are determined from additional assumptions such as smooth (derivatives) and sparse (number of components).

Inversion using SVD and $\mathbf{L}^2$-minimization

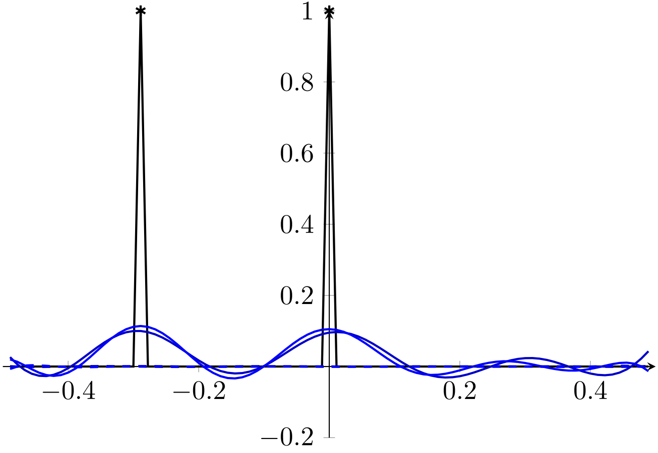

Solution using SVD and $\mathbf{L}^2$. The current spread around the original source positions.

$\mathbf{L}^p$ for the unresolved components

The $\mathbf{L}^2$ inversion indicates a resolution of the order $\lambda/4$ to $\lambda/2$.
The resolved part can be determined from the observations $\mathbf{A}\mathbf{x} = \mathbf{b}$.
Regularization with just two components satisfying $x_1 + x_2 = 1$ (from $\mathbf{A}\mathbf{x} = \mathbf{b}$)

$$\min\|\mathbf{x}\|_2^2 = x_1^2 + x_2^2 = 0.5 \quad \text{for } x_1 = x_2 = 0.5$$

and

$$\min\|\mathbf{x}\|_1 = |x_1| + |x_2| = 1 \quad \text{for any } x_1, x_2 \geq 0$$

If x_1 fits the data slightly better than x_2.

- $\mathbf{L}^2$ regularization produces $x_1 \approx x_2 \approx 0.5$. A smooth image with features determined by the resolution.
- $\mathbf{L}^1$ regularization produces $x_1 \approx 1$ and $x_2 \approx 0$. Good for sparse cases (few dominant components) but otherwise irregular random results.

$\mathbf{L}^1$-regularization

Change of the $\mathbf{L}^2$-regularization to $\mathbf{L}^1$ gives the optimization problem

$$\text{minimize} \|\mathbf{A}\mathbf{x} - \mathbf{b}\|_2 + \alpha\|\mathbf{x}\|_1 \tag{1}$$

Can also be formulated as

$$\begin{aligned} \text{minimize} \quad & \|\mathbf{x}\|_1 \\ \text{subject to} \quad & \|\mathbf{A}\mathbf{x} - \mathbf{b}\|_2 \leq \delta, \end{aligned} \tag{2}$$

where the parameter δ can be estimated from the SVD solution $\delta \approx \|\mathbf{A}\mathbf{x}_{\text{SVD}} - \mathbf{b}\|_2$. This formulation tries to produce a solution with similar fit to the data as the SVD ($\mathbf{L}^2$) but without the smoothing (a few dominant components).

Inversion using SVD, $\mathbf{L}^2$, and $\mathbf{L}^1$-minimization

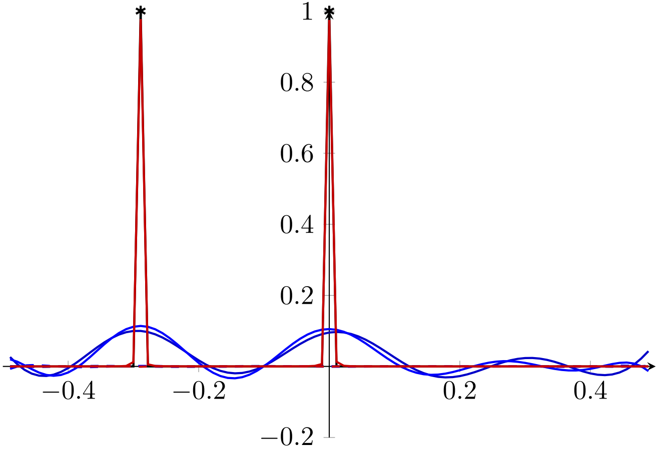

Change from $\mathbf{L}^2$ (blue) to $\mathbf{L}^1$ (red) regularization. It correctly finds the original sources. Note the inverse crime as $\mathbf{A}$ was used to create the data.

Inversion using SVD, $\mathbf{L}^2$, and $\mathbf{L}^1$-minimization

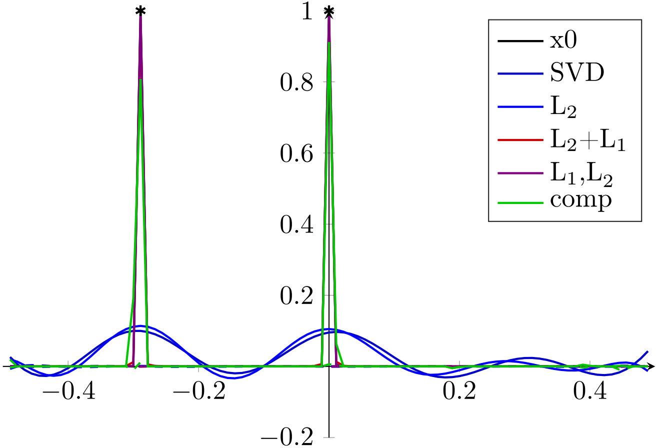

The number of measurements should be compared to number of non-zero components in compressed sensing, here $M = 80$ is reduced to $M = 19$ (green).

Planar case

$$\mathbf{b} = \mathbf{A}_1\mathbf{x}_1 + \mathbf{A}_2\mathbf{x}_2$$

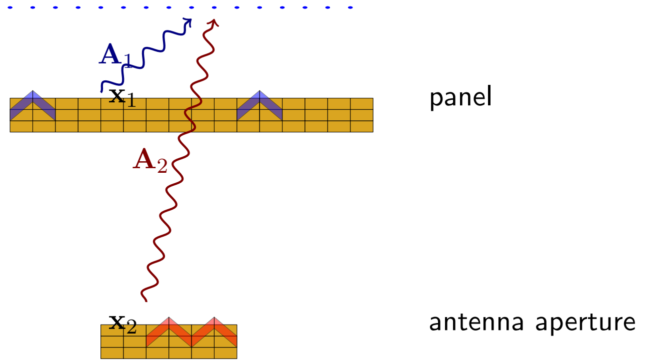

- $51^2 = 2601$ sample points (λ separation)
- $100^2 = 10000$ basis function ($\lambda/2$ separation)
- linear polarization
- antenna 120λ to panel 12λ to observations

Planar case

Observed (measured) field (antenna and 10 defects)

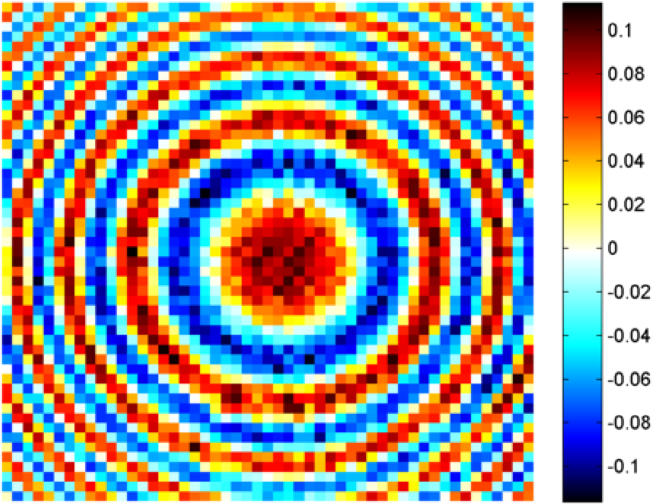

Source separation

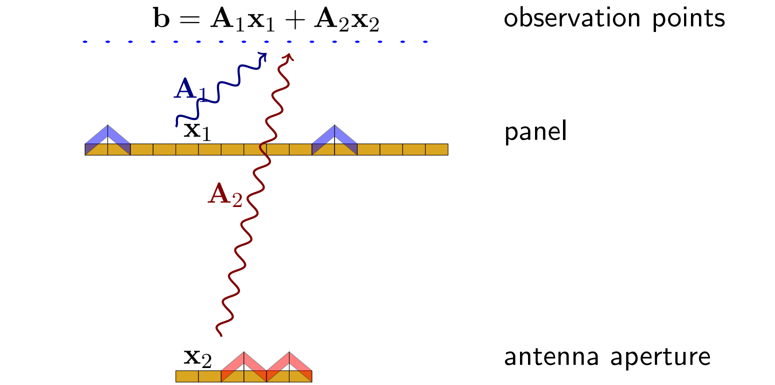

Regularize by minimizing $\mathbf{x}_1$, *i.e.*,

$$\begin{aligned} &\text{minimize} && \|\mathbf{x}_1\|_1 \\ &\text{subject to} && \|\mathbf{A}_1\mathbf{x}_1 + \mathbf{A}_2\mathbf{x}_2 - \mathbf{b}\|_2 \leq \delta. \end{aligned}$$

Also add constraints $\|\mathbf{B}\mathbf{x}_2\|$ to suppress superdirectivity.

Planar case

Subtracted field from the antenna aperture

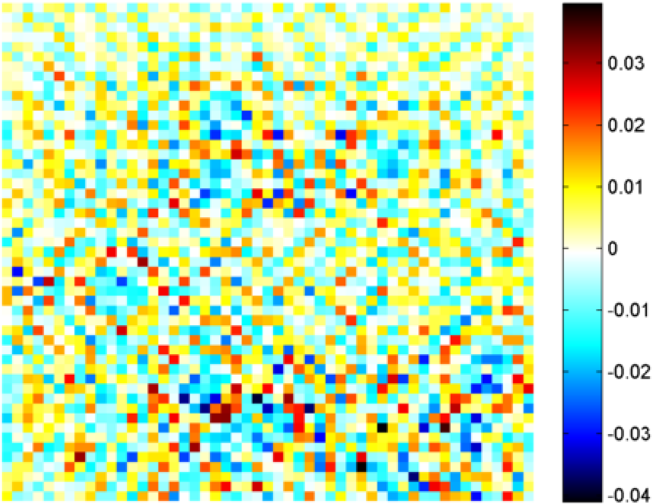

Matrix-free algorithms

The computational complexity can be prohibitive for larger problems, *e.g.*, the rather coarse discretization of 100×100 unknowns corresponds to a matrix $\mathbf{A}$ with 10^8 elements.
Cannot store the matrix explicitly but can evaluate $\mathbf{A}\mathbf{x}$ and $\mathbf{A}^{\mathsf{H}}\mathbf{b}$ efficiently.
Often efficient to utilize (translational) symmetries and FFT based algorithms to reduce the computational complexity.

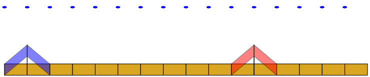

Using the same spacing for the basis functions and the data points gives a (block) Toeplitz matrix

Toeplitz matrix vector multiplication

Let $M=N$ and embed the $M\times M$ Toeplitz matrix into a $2M\times 2M$ circulant matrix such that

$$\begin{pmatrix}\mathbf{A}\mathbf{x}\\ \mathbf{S}\mathbf{x}\end{pmatrix}=\begin{pmatrix}\mathbf{A} & \mathbf{S}\\ \mathbf{S} & \mathbf{A}\end{pmatrix}\begin{pmatrix}\mathbf{x}\\ \mathbf{0}\end{pmatrix}$$

The circulant matrix $\tilde{\mathbf{A}}$ has the first row

$$\tilde{\mathbf{A}}_{1,:}=\begin{pmatrix}A_{11} & A_{21} & \cdots & A_{M1} & 0 & A_{1N} & \cdots & A_{12}\end{pmatrix}$$

Evaluate using the FFT, *i.e.*, from the first M elements of, *i.e.*,

$$\mathbf{A}\mathbf{x}=[\mathcal{F}^{-1}(\mathcal{F}(\tilde{\mathbf{A}}_{1,:})\mathcal{F}([\mathbf{x}\ \mathbf{0}]))]_{1:M}$$

Can reduce the dimension to $M+N-1$

$$\tilde{\mathbf{A}}_{1,:}=\begin{pmatrix}A_{11} & A_{12} & \cdots & A_{1N} & 0 & A_{M1} & \cdots & A_{21}\end{pmatrix}$$

or $M+N+P-1$ where $P\geq 0$ is the number of additional zeros.

Planar case

Observed (measured) field (antenna and 10 defects)

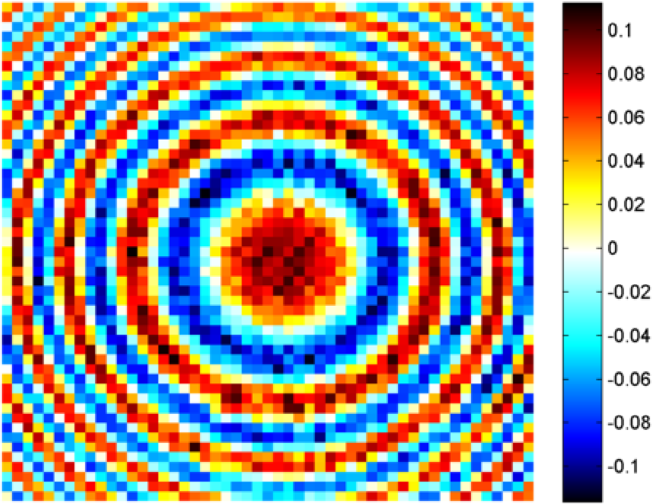

Planar case

Subtracted field from the antenna aperture

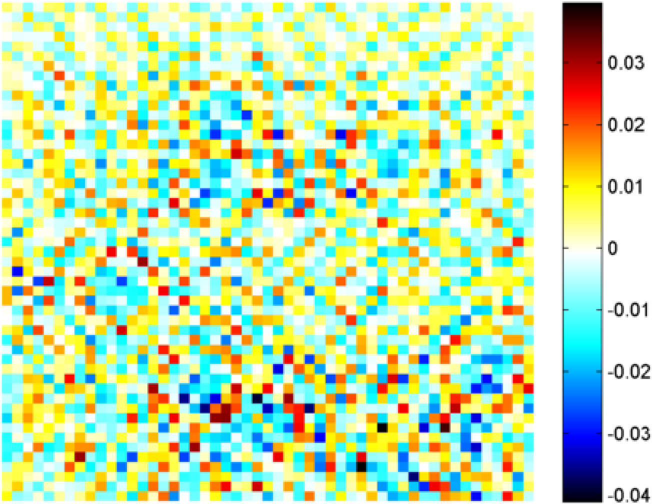

Planar case

Back propagation using the adjoint

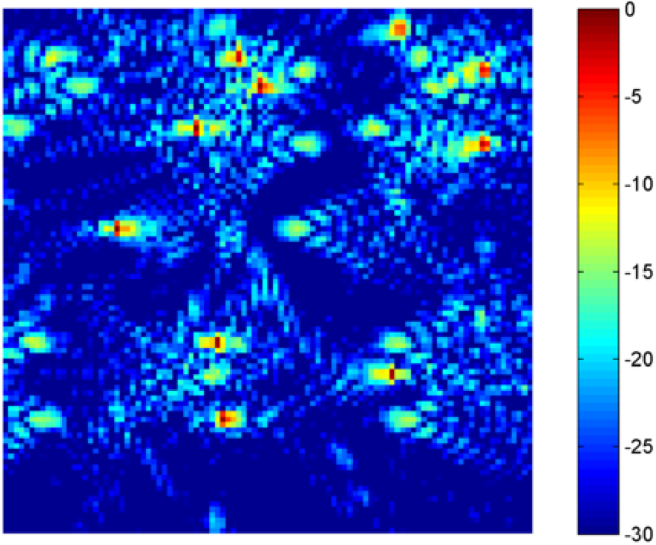

Planar case

$\mathbf{L}^1$ with 20% of the data

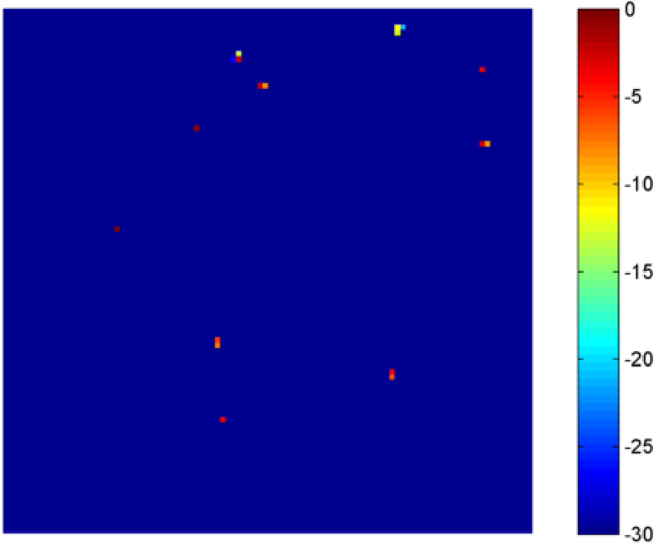

Planar scan at $60\,\mathrm{GHz}$: Synthetic data

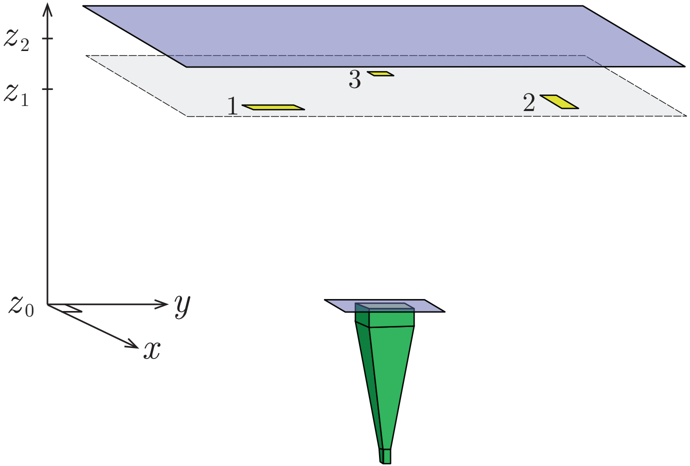

Simulation (FEKO) setup with 3 defects: side view

Planar scan at $60\,\mathrm{GHz}$: Synthetic data

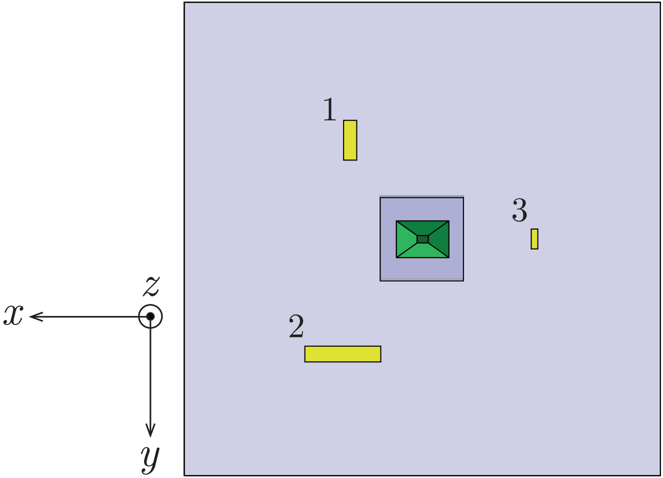

Simulation (FEKO) setup with 3 defects: top view

Planar scan at $60\,\mathrm{GHz}$: Synthetic data

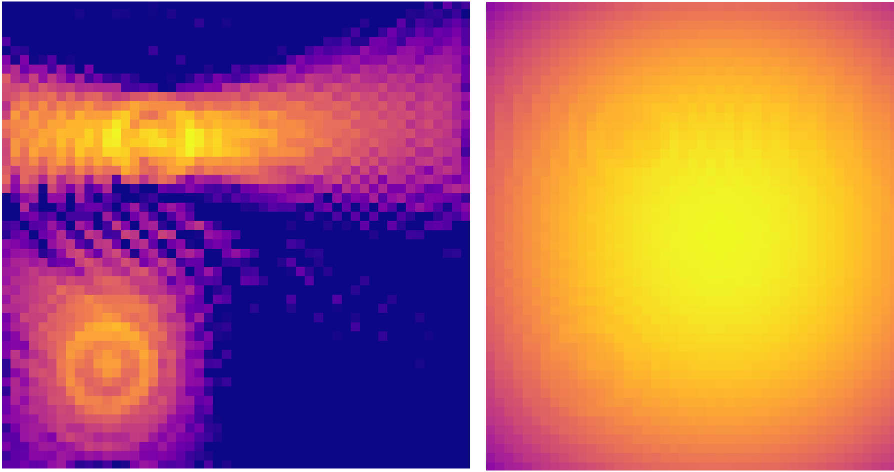

(left) scattered field (right) total field

Planar scan at $60\,\mathrm{GHz}$: Synthetic data

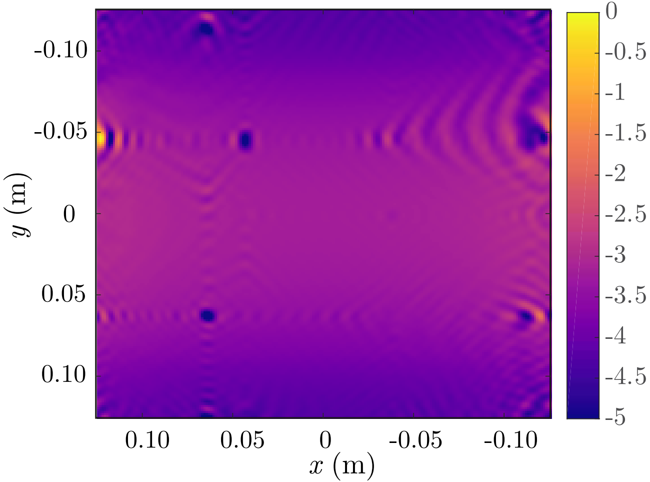

Back propagation with background subtraction $5\,\mathrm{dB}$

Planar scan at $60\,\mathrm{GHz}$: Synthetic data

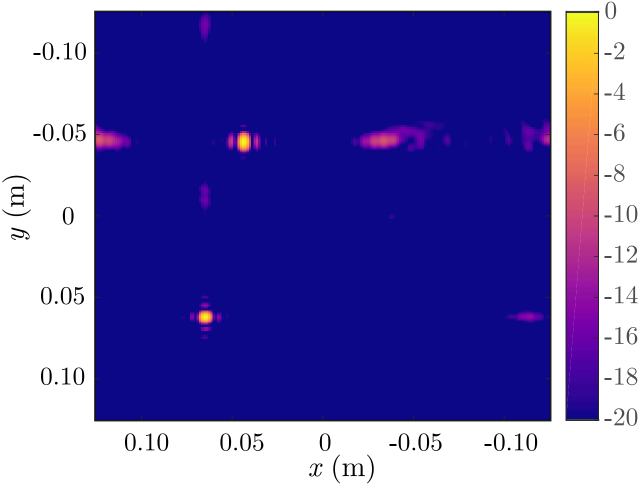

Back propagation with source separation $20\,\mathrm{dB}$

Planar scan at $60\,\mathrm{GHz}$: Synthetic data

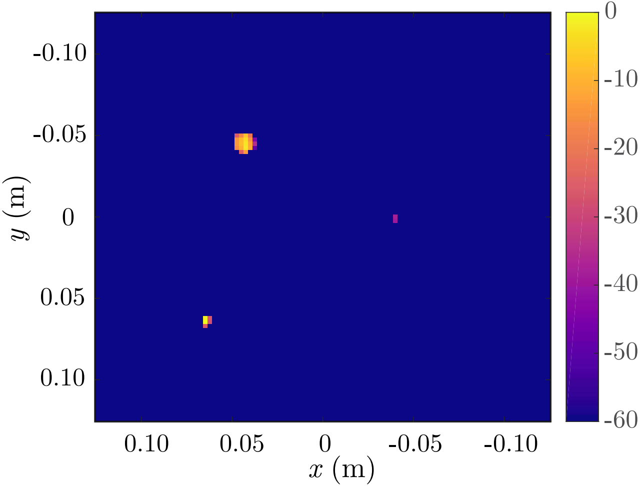

Compressive sensing with source separation $60\,\mathrm{dB}$

Planar scan at $60\,\mathrm{GHz}$: Synthetic data

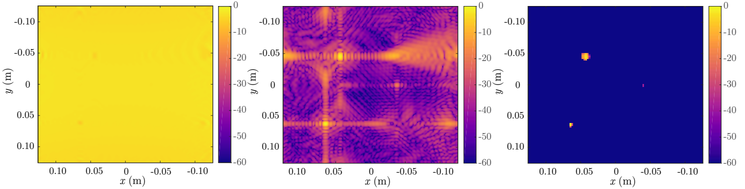

(left to right) back propagation, source separation, CS $60\,\mathrm{dB}$

Planar scan at $60\,\mathrm{GHz}$

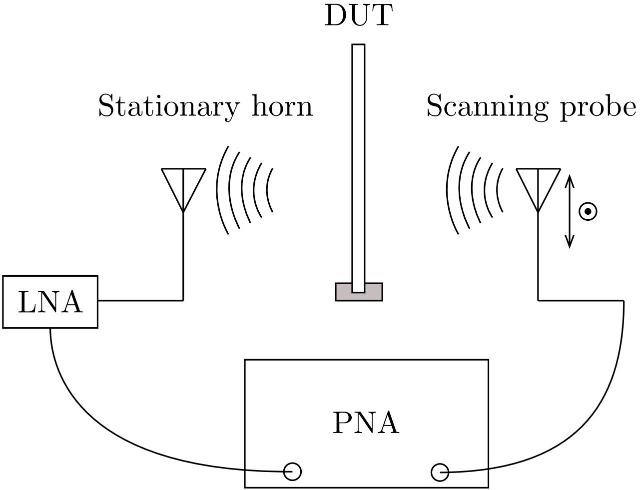

Planar scan at $60\,\mathrm{GHz}$

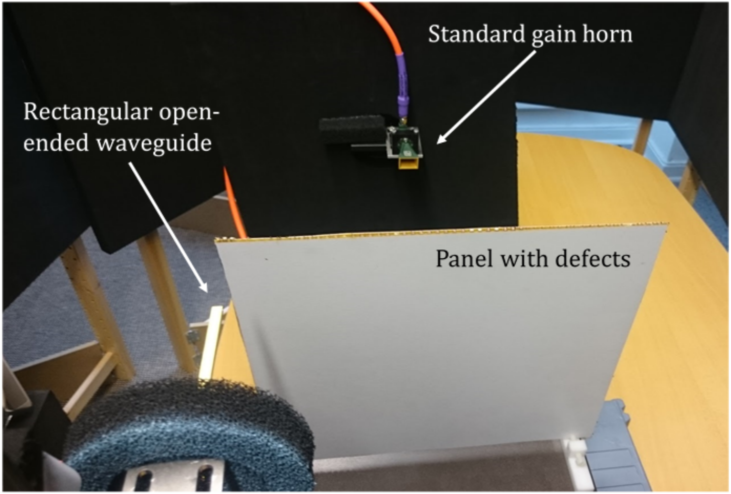

Planar scan at $60\,\mathrm{GHz}$

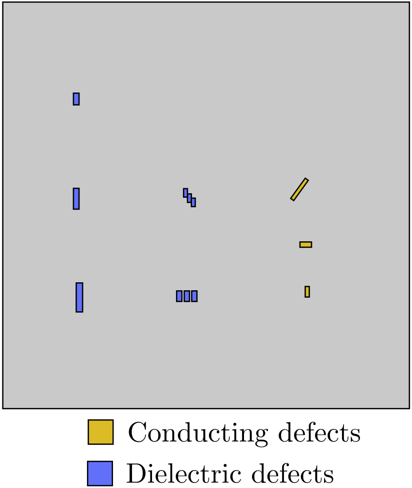

Planar scan at $60\,\mathrm{GHz}$

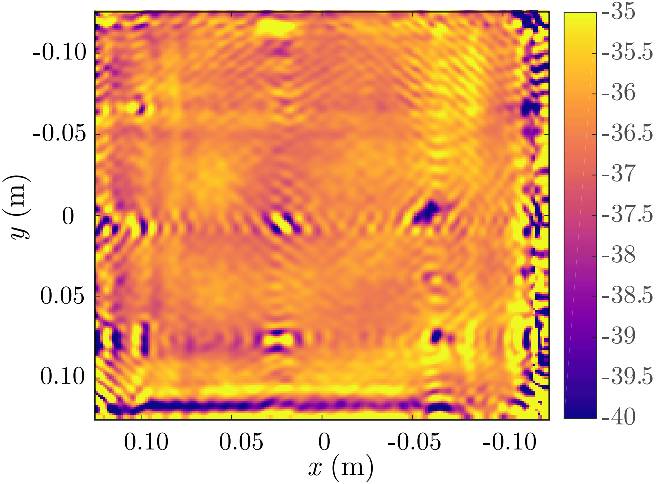

Back propagation with background subtraction $5\,\mathrm{dB}$

Planar scan at $60\,\mathrm{GHz}$

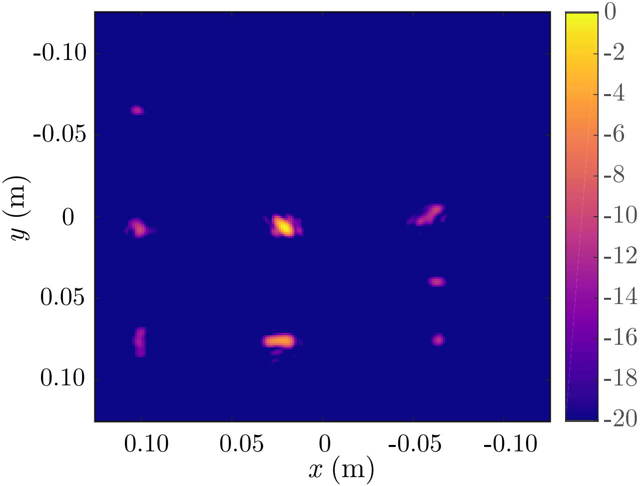

Back propagation with source separation $20\,\mathrm{dB}$

Planar scan at $60\,\mathrm{GHz}$

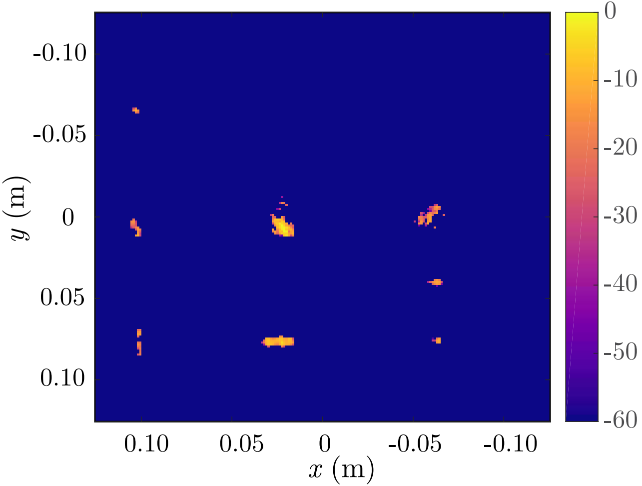

Compressive sensing with source separation $60\,\mathrm{dB}$

Planar scan at $60\,\mathrm{GHz}$

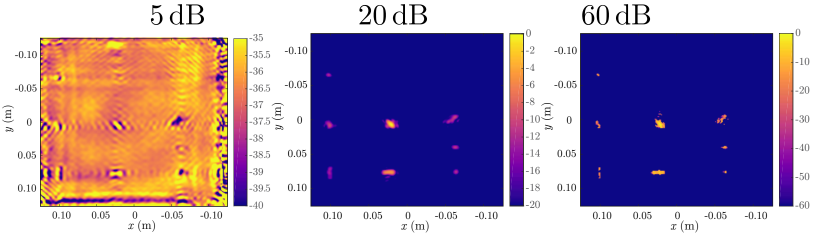

Back propagation, source separation, compressive sensing

Helander *etal*, 'Imaging using Compressive Sensing Techniques for Planar Non-Destructive Testing at $60\,\mathrm{GHz}$', 2017.

Outline

1. **Acknowledgments & Lund University**
2. **Motivation**
3. **Radome and Antenna diagnostics**
   - Inverse source problem
   - Inversion algorithm
   - Radome diagnosticss
4. **Compressive sensing**
5. **Conclusions**

Summary

- Imaging of near fields and/or equivalent currents can localize defects and help understanding.
- Integral equations/representations (similar to MoM) for EM modeling.
- Applications for radome diagnostics, antenna diagnostics, near- to far-field transformations, and post processing of measurement data.
- The first commercial packages (TICRA and Microwave Vision Group) were released 2011.
- Much research remains in understanding of algorithms, regularization, and imaging quality.
- Use of different norms *e.g.*, L_1, compressive sensing,...

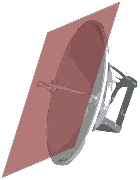

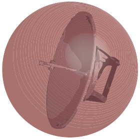

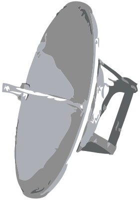

Slides: `http://www.eit.lth.se/staff/mats.gustafsson`

References I

Araque Quijano, J. L. A., L. Scialacqua, J. Zackrisson, L. J. Foged, M. Sabbadini, and G. Vecchi (2011). "Suppression of undesired radiated fields based on equivalent currents reconstruction from measured data". *Antennas and Wireless Propagation Letters, IEEE* 10, pp. 314–317.

Foged, L. J., L. Scialacqua, F. Saccardi, J. L. Araque Quijano, G. Vecchi, and M. Sabbadini (2012). "Practical application of the equivalent source method as an antenna diagnostics tool". *IEEE Antennas Propag. Mag.* 54.5, pp. 243–249.

Gustafsson, M., M. Sebesta, B. Bengtsson, S.-G. Pettersson, P. Egelberg, and T. Lenart (2004). "High resolution digital transmission microscopy—a Fourier holography approach". *Optics and Lasers in Engineering* 41.3, pp. 553–563.

Hansen, P. C. (2008). "Regularization Tools, version 4.1 for Matlab 7.3". *Numerical Algorithms* 46, pp. 189–194.

— (2010). *Discrete inverse problems: insight and algorithms*. Vol. 7. Society for Industrial & Applied.

Helander, J., A. Ericsson, M. Gustafsson, T. Martin, D. Sjöberg, and C. Larsson (2017). *Imaging using Compressive Sensing Techniques for Planar Non-Destructive Testing at 60 GHz*. Tech. rep. LUTEDX/(TEAT-7245)/1–21/(2017). Lund University.

Jörgensen, E., D. W. Hess, P. Meincke, O. Borries, C. Cappellin, and J. Fordham (2012). "Antenna diagnostics on planar arrays using a 3D source reconstruction technique and spherical Near-Field measurements". In: *Antennas and Propagation (EUCAP), Proceedings of the 6th European Conference on*. IEEE, pp. 2547–2550.

Massa, A., P. Rocca, and G. Oliveri (2015). "Compressive Sensing in Electromagnetics-A Review". *IEEE Antennas Propag. Mag.* 57.1, pp. 224–238.

Persson, K. and M. Gustafsson (2005). "Reconstruction of equivalent currents using a near-field data transformation – with radome applications". *Prog. Electromagn. Res.* 54, pp. 179–198.

Persson, K., M. Gustafsson, G. Kristensson, and B. Widenberg (2013). "Source reconstruction by far-field data for imaging of defects in frequency selective radomes". *IEEE Antennas and Wireless Propagation Letters* 12, pp. 480–483.

Persson, K., M. Gustafsson, G. Kristensson, and B. Widenberg (2014). "Radome diagnostics — source reconstruction of phase objects with an equivalent currents approach". *IEEE Trans. Antennas Propag.* 62.4.

Tarantola, A. (2005). *Inverse problem theory and methods for model parameter estimation*. Society for Industrial and Applied Mathematics.